

# Conduction mechanisms near the metal–insulator transition range

V. F. Gantmakher, V. N. Zverev, V. M. Teplinskii, and O. I. Barkalov

*Institute of Solid State Physics, Russian Academy of Sciences*

(Submitted 3 December 1992)

Zh. Eksp. Teor. Fiz. **103**, 1460–1475 (April 1993)

A study is presented of the interchange between the (intrinsically different) Boltzmann, hopping, and—in the critical region—scaling conduction mechanisms near a metal–insulator transition. For the case when the electron–electron interaction governs the conduction mechanism in this vicinity, an analog of a phase diagram is constructed for the transition, based on data obtained for Cd–Sb alloy in the process of its amorphization. A quasireentrant superconducting-transition line is also shown on the diagram.

## 1. INTRODUCTION

Near the metal–insulator (MI) transition, intrinsically different conduction mechanisms compete and change one into another. In this paper an analog of a phase diagram for this vicinity is constructed on the basis of experimental data obtained from a Cd–Sb alloy<sup>1,2</sup> during its amorphization. The purpose of the diagram is to illustrate the relationship between the coexistence domains of various conduction mechanisms in the MI transition range at finite temperatures.

It is known that the MI transition is defined by the vanishing of the conductivity  $\sigma(0)$  at temperature  $T = 0$ . Since there are a variety of “metallicity parameters” indicative of the distance from the transition (such as impurity concentration,<sup>3</sup> the degree of disorder,<sup>4</sup> the band overlap, etc.), the motion through the phase space of the system often implies a change, or changes, from one material to another. It happens only rarely that the MI transition can be passed through in a reversible manner, by just varying some external parameters rather than the properties of the sample. For example, one can pass the transition by varying the magnetic field applied to the system—and thereby changing the overlap of the impurity-localized electronic wave functions.<sup>5,6</sup> Even then, however, no singularities in either specific heat or any other thermodynamic function are involved, and one must extrapolate the temperature dependences  $\sigma(T)$  to  $T = 0$  to establish the occurrence of the transition.

At finite temperatures, varying the metallicity parameter enables one to bypass a phase transition when changing from the  $M$  to the  $I$  state, in much the same manner as a change from a liquid to a gaseous state may be performed without a phase transition. To describe this bypass path, the vicinity of the transition in an appropriately constructed phase space must be analyzed.

All transitions depend on much the same concepts for their statistical description. One of these is the correlation length  $\xi$ , a statistical quantity divergent on both sides of the transition.<sup>7</sup> As a measure of the proximity to the transition we use a quantity  $f$ , defined as  $f = 1/\xi$  on the  $I$  side and as  $f = -1/\xi$  on the  $M$  side of the transition. Let us investigate the vicinity of the MI transition on the  $(f, T)$ -plane shown in Fig. 1. The origin of the coordinate system is taken to be at the transition point  $\sigma(0) = 0$  on the horizontal axis  $T = 0$ . If the motion of the system along the  $f$  axis is due to the variation in the degree of disorder, then we are dealing with what is known as the Anderson transition.<sup>8</sup> Variation of the density of electronic states results in a Mott transition.<sup>9</sup> The

parameter  $1/\xi$  is useful in either case. In the  $I$  region it is interpreted as the localization radius of the wave functions at the Fermi level.<sup>10</sup>

We ignore the possibility of a superconducting transition for the moment, and discuss only the normal conduction regime at various points of the  $(f, T)$ -plane.

Far enough on the  $M$  side of the transition we have a Boltzmann conductivity modified by quantum corrections:<sup>11</sup>

$$\sigma(T) = \sigma_0(T) + \Delta\sigma(T) = \frac{1}{3\pi^2} \frac{e^2}{\hbar} k_F(k_F l(T)) + \frac{e^2}{\hbar} \frac{1}{L(T)}, \quad (1)$$

$$\sigma_0 \gg \Delta\sigma, \quad (2)$$

where  $k_F$  is the Fermi wave vector,  $l$  the mean free path, and  $L$  the phase relaxation length of the wave function. In terms of the diffusion coefficient  $D$  and the phase relaxation time  $\tau_\varphi$ :

$$L = (D\tau_\varphi)^{1/2}. \quad (3)$$

Deep inside the  $I$  region we are in the hopping regime with

$$\sigma \propto \exp[-(T_m/T)^{1/m}], \quad (4)$$

where  $T_m$  is a parameter and  $1/m$  is, in three dimensions, either  $1/4$  (Mott's law<sup>12</sup>) or  $1/2$  (Shklovskii–Éfros' law<sup>13</sup>).

The central, or small  $1/\xi$ , part of the diagram belongs to the so-called critical, or scaling, regime.<sup>7</sup> In this region the inequality (2) is reversed, indicating that the conductivity is largely quantum-mechanical in character. The scaling region may be subdivided into  $M$  and  $I$  subregions lying on the opposite sides of the  $f = 0$  axis. Either of these will be considered separately further below. First, however, a brief description of our experimental background will be given.

## 2. EXPERIMENT

The experimental data used in this study were obtained from the Cd<sub>43</sub>Sb<sub>57</sub> alloy in the process of amorphization of its high-pressure metastable  $M$  phase. While this phase may persist arbitrarily long at nitrogen temperatures, heating to room temperatures irreversibly transforms it into an amorphous  $I$  phase.<sup>14</sup> By stepwise heating one can repeatedly interrupt this process to obtain a sequence of intermediate quasistable states in one and the same sample at certain below-room temperature. Refs. 1 and 2 give a detailed discussion of this procedure as well as of the transport and su-

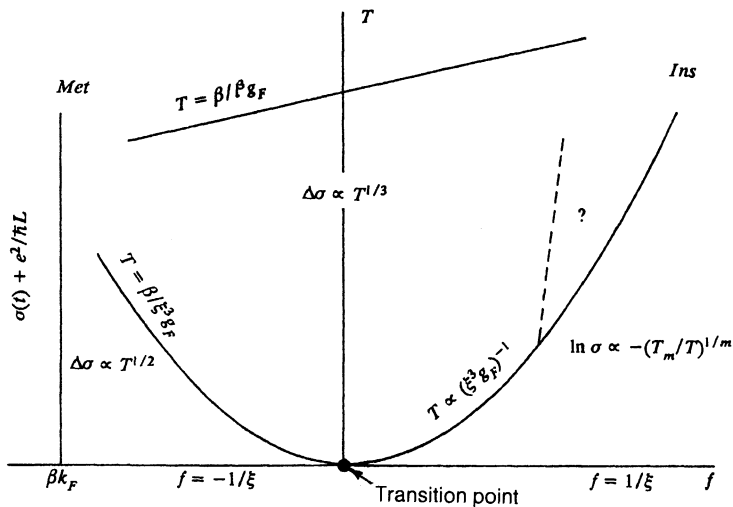


FIG. 1. Conduction mechanisms in the vicinity of the metal-insulation transition (schematic).

perconducting properties of the series of states so obtained. The same references present arguments intended to show that the initial material is homogeneous and has only small element-density spatial fluctuations (these fluctuations being the main "external" source of inhomogeneity of an amorphous material). Specifically, these arguments are the  $\sigma \propto T^{1/3}$  dependence observed over a wide range of the states,<sup>1</sup> and the narrow superconducting transition occurring at one of the amorphization stages (Figs. 1 and 2 in Ref. 2). Needless to say, these arguments do not actually prove the homogeneity property, nor do they permit any quantitative estimates.

In Ref. 2 the states of the sample in the above sequence were indexed by the logarithm of the resistivity ratio measured at  $T = 6$  K:

$$q = \lg(R/R_0)_{T=6 \text{ K}}, \quad (5)$$

where  $R_0$  is the resistivity of the sample in the initial state. The results we present here were obtained in the same series of experiments. The MI transition occurred at  $q = 3.9$ .

Unlike in Ref. 1, in the present study the dependence  $\sigma(T)$  was measured in a magnetic field  $H = 4$  T in order to eliminate superconducting interaction effects. Comparison of the  $R(T)$  dependences obtained with and without field

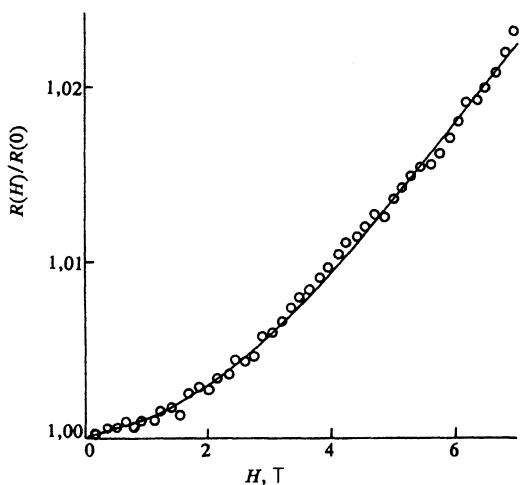


FIG. 2. Magnetoconductivity for the  $q = 4.9$  state at  $T = 4.2$  K.

reveals a relatively small magnetoresistance for  $T > 4$  K. In the  $q = 4.9$  state, for example, application of a magnetic field  $H = 4$  T at  $T = 4.2$  K increases  $R$  by 1% (Fig. 2), as against the twofold increase due to a temperature rise from 4 to 10 K.

### 3. METALLIC PART OF THE SCALING REGION

As the MI transition is approached from its metallic side at  $T = 0$ , the product  $k_F l$  decreases and tends to unity while the conductivity  $\sigma(0)$  approaches its minimum Boltzmann value

$$\sigma(0) \rightarrow \sigma_{min} = \gamma \frac{e^2}{\hbar} k_F = \gamma \frac{e^2}{\hbar} \frac{1}{l},$$

where  $\gamma$  replaces the free-electron factor  $1/3\pi^2$  of Eq. (1). N. Mott, the author of the concept of a minimum metallic conductivity,<sup>15</sup> suggested a rather close value  $\gamma = 0.026$ . The condition

$$-f = \gamma k_F \quad \text{or} \quad 1/\xi = \gamma k_F = \gamma/l \quad (6)$$

yields the left boundary for the scaling region shown in Fig. 1. To the right of the boundary, the physical meaning of the length parameter entering the conductivity expression changes. In the scaling region this length does not represent the mean free path but is rather the correlation length

$$\sigma(0) = \gamma \frac{e^2}{\hbar} \frac{1}{\xi} \quad (7)$$

and the conductivity in this region is less than  $\sigma_{min}$ :

$$\sigma < \sigma_{min}, \quad \xi > 1/k_F.$$

At finite temperatures one more parameter with the dimensions of length comes into play: the length  $L$  defined by Eq. (3) and dependent on inelastic interactions. In the left portion of the scaling region the conductivity is usually interpolated by<sup>10</sup>

$$\sigma(T) = \sigma(0) + \beta \frac{e^2}{\hbar} L^{-1}(T), \quad (8)$$

where the constant  $\beta = 2/3\pi^3 \approx 0.022$  calculated by Kawabata,<sup>16</sup> differs little from both the constant 0.026 in Mott's  $\sigma_{min}$  expression<sup>15</sup> and the factor  $(3\pi^2)^{-1}$  in (1). In what follows we put  $\gamma = \beta$  to be able to match the lengths due to

appear in the analysis. A change in  $\gamma$  has no other effect than to modify the  $\xi$  scale.

We restrict ourselves to the case of a critical regime dominated by the  $e$ - $e$  interaction<sup>11</sup>

$$\tau_\varphi = \tau_{ee} = \hbar/T, \quad L = L_{ee} = (D\hbar/T)^{1/2}$$

(from here on,  $T$  is measured in ergs, i.e., the Boltzmann constant  $k_B = 1$ ). Substituting  $L_{ee}$  into (8) and using the Einstein relation

$$\sigma = e^2 g_F D \quad (9)$$

( $g_F$  being the density of states at the Fermi level), we obtain the equation

$$x^{3/2} = x^{1/2} + t^{1/2} \quad (10)$$

expressed in the dimensionless units

$$x = \sigma(T)/\sigma(0), \quad t = T/T^*, \quad T^* = \left( \frac{\sigma(0)}{e^2/\hbar} \right)^3 \frac{1}{\beta^2 g_F} = \frac{\beta}{\xi^3 g_F}.$$

If  $T \gg T^*$  then  $\sigma(T) \gg \sigma(0)$ , and the solution to Eq. (10) takes the form

$$x = \frac{2}{3} + t^{1/3}, \quad \sigma = \frac{2}{3} \sigma(0) + \frac{e^2}{\hbar} (\beta^2 g_F T)^{1/3}. \quad (11)$$

The dependence  $\Delta\sigma \propto T^{1/3}$  has been observed many times experimentally.<sup>4-6,17-19,1</sup> In the opposite extreme case  $T \ll T^*$  we have

$$x = 1 + t^{1/2}, \quad \sigma(T) = \sigma(0) + T^{1/2} \left( \frac{e^2}{\hbar} \right)^{3/2} \frac{\beta g_F^{1/2}}{\sigma(0)}. \quad (12)$$

Equation (12) is of the same form as Eq. (1) for the quantum-corrected Boltzmann conductivity,

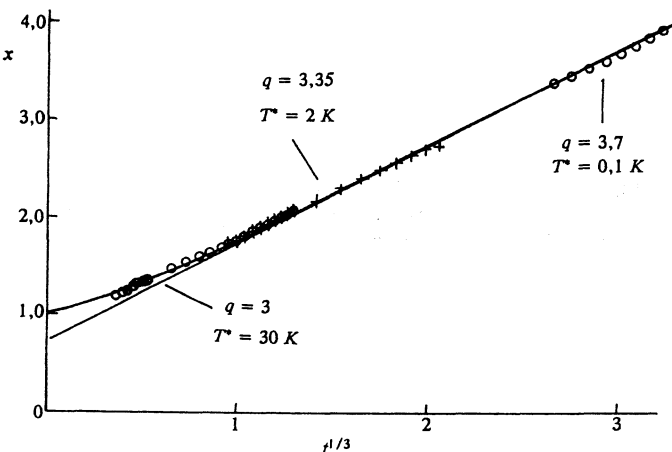
$$\sigma = a + bT^{1/2}. \quad (13)$$

What makes the difference, however, is that the main term  $\sigma(0)$  in (12) can no longer be described by the electron-gas model but is rather of a quantum-mechanical nature, just as the second term,  $\Delta\sigma \propto T^{1/2}$ .

The equation  $T = T^*$ , i.e.,

$$T = \beta/g_F \xi^3, \quad (14)$$

defines the dividing line in the scaling region of the diagram



of Fig. 1. If  $g_F$  does not change from one state to another (Anderson transition), the  $T \propto (1/\xi)^3$  along this line. Note that  $g_F$  may depend on  $f$ , however.

We now turn to the experimental data. For the states  $3 < q < 3.9$ , immediately on the  $M$  side of the transition, a comparison of the  $\sigma(T)$  dependences with the universal curve (10) was made to determine the state parameters  $\sigma(0)$  and  $T^*$  [see Fig. 3 and Table I]. The state  $q = 3.9$  is close enough to the transition to use the asymptotic expression (11) when determining  $\sigma(0)$  and  $g_F$ . The results permit real-scale ( $f, T$ )-diagrams to be plotted (see Fig. 9 below).

Since the correlation length  $\xi \propto [\sigma(0)]^{-1}$ , it follows from the three upper rows of the table that the true  $T^*(\xi)$  dependence is closer to  $T^* \propto \xi^{-2}$  than to  $T^* \propto \xi^{-3}$ . This is accounted for by changes in  $g_F$ . The evolution of the density of states is thus an independent factor affecting the nature of the transition.

For the boundary state near the MI transition, the value of  $g_F$  differs by a factor of about 10 from that for another sample,<sup>1</sup> indicative of an approximately twofold spread in the conductivity of boundary-state samples. This, we presume, is due to uncertainties in determining geometrical factors for irregularly shaped samples.

#### 4. INSULATING PART OF THE SCALING REGION

On crossing over from the  $M$  into  $I$  subregion along the  $f$  axis at moderately low temperatures, the functional dependence of the type (11),

$$\sigma = a + bT^{1/3} \quad (15)$$

remains unchanged, but this time  $a < 0$ .<sup>6,1</sup> This has to do with the fact that as the temperature is lowered, a transition from the critical to the hopping regime must occur. This is illustrated in Fig. 4.

The question of the existence of a Coulomb gap—and hence the question of the exponent  $1/m$  in (4)—is usually answered by analyzing the experimental  $R(T)$  dependence, the temperature range being taken as wide as possible for the purpose.<sup>3,20</sup> In the present study the temperature range is bounded from above by our assumption that at  $T \simeq 2$ – $3$  K the scaling regime sets in. Figure 5 shows in a semilogarithmic scale the temperature dependences for  $T < 3$  K for the same states as in Fig. 4. The straight-line plots of Fig. 5a imply that the obtained results are describable in terms of the Mott law.

FIG. 3. The universal function, Eq. (10), and its linear asymptotic form, Eq. (11). Experimental points represent the states  $q = 3, 3.35$ , and  $3.7$ .

TABLE I.

$q$	3	3,35	3,7	3,9	4	4,3	4,7	4,9
$g_F$ , $\text{erg}^{-1}\text{cm}^{-3}$	$8 \cdot 10^{30}$	$2,5 \cdot 10^{30}$	$7 \cdot 10^{29}$	$3 \cdot 10^{29}$	$2 \cdot 10^{29}$	$4 \cdot 10^{28}$	$5 \cdot 10^{27}$	$2,5 \cdot 10^{27}$
$\sigma(0)$ , $\text{Ohm}^{-1}\text{cm}^{-1}$	6,1	1,7	0,34	0				
$T^*$ , K	30	2	0,1					
$T_4/T_2$ , K							140/1,7	320/3
$T_{c0}$ , K	3,65	3,78	3,75	3,76	3,72	3,68	3,65	3,63

The state parameter  $q^*$  is defined in (5);  $g_F$ , the density of states at the Fermi level, is defined by the slope of the straight-line plots of  $\sigma(T^{1/3})$ ;  $\sigma(0)$  and  $T^*$  (relevant only for  $q > 3.9$ , the  $M$  part of the table) are found by setting the scale for the dimensionless units  $x$  and  $t$  on the universal graph of Fig. 2;  $T_4$  and  $T_2$  are determined from the graphs of Fig. 5;  $T_{c0}$  values are taken from Ref. 2 (see also inset in Fig. 7).

It is worthwhile, however, to take a closer look at the  $T_4$  values obtained. Noting that the permittivity diverges as

$$\kappa = \kappa_0 + 4\pi e^2 g_F \xi^2, \quad (16)$$

in the vicinity of the MI transition, it can be shown (see a review article by Castner<sup>3</sup>) that the constants  $T_4$  and  $T_2$  and the Coulomb gap  $\Delta$  scale with  $\xi$  like

$$T_4/T_2 \approx 80, \quad T_4/\Delta \approx 800. \quad (17)$$

The second of these estimates suggests a Coulomb gap of order  $\Delta \approx 0.2-0.4$  K in these states. The average hopping energy in the presence of a Coulomb gap is<sup>3,13</sup>

$$\bar{\Delta}_2 \approx \frac{1}{2} (TT_2)^{1/2} \approx 1,6(T\Delta)^{1/2},$$

so that the Shklovskii-Éfros law can only be obeyed for  $T < \Delta/2$ . It is not surprising therefore that it is only at the lowest temperatures that the  $\log\sigma(T^{1/2})$  curves asymptote into straight lines as shown in Fig. 5b. Note, however, that the slope of the straight lines is correct in the sense of being consistent with the first of the estimates (17).

In order to describe the lower boundary of the scaling region let us note that variable-range hopping conduction occurs when

$$r_m > \xi, \quad (18)$$

where  $r_m$  is the hopping length. If  $m = 4$  (Mott's law), then<sup>3</sup>

$$r_4 = \frac{3}{8} \xi \left( \frac{T_4}{T} \right)^{1/4}, \quad T_4 = 18(g_F \xi^3)^{-1},$$

and the boundary of the scaling region is given, to within a numerical factor, by equation (14) encountered in the  $M$  region.

When the Coulomb gap becomes significant, so that Shklovskii-Éfros hopping conduction with  $m = 2$  takes place, we have

$$r_2 = \frac{1}{4} \xi \left( \frac{T_2}{T} \right)^{1/2}, \quad T_2 = 2,8 \frac{e^2}{\kappa \xi}.$$

Substituting (16) for  $\kappa$  we again arrive at (14), but with a coefficient  $2.8/4\pi \approx 0.22$  instead of 18.

Thus Eq. (14) is a correct functional dependence of the boundary temperature  $T^*$  on  $\xi$  and  $g_F$  in the  $I$  region. We note, however, that the numerical factor in (14) is dependent on the particular hopping conduction model being used. We also note that, in contrast to the  $M$  region, we have not independent method for determining  $\xi$ . In particular, there is as yet no model capable to relate  $\xi$  to the absolute value of the constant  $\alpha$  in expression (15) for the  $I$  region. Experiment shows that  $\alpha$  is a monotonic function of  $q$ , see Fig. 6.

This problem gives rise to another one. According to Ref. 1, a change from (15) to  $\Delta\sigma \propto T^{1/2}$  occurs not only on moving in the  $M$  direction, but in the  $I$  direction as well. This

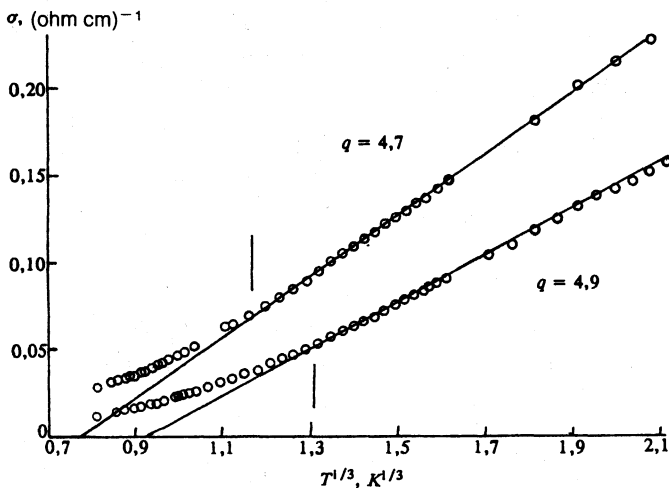


FIG. 4. Variation of  $\sigma$  with  $T^{1/3}$  for the states  $q = 4.7$  and  $4.9$  in a magnetic field  $H = 4$  T. Vertical bars indicate temperatures at which a systematic deviation of experimental points from straight-line plots begins.

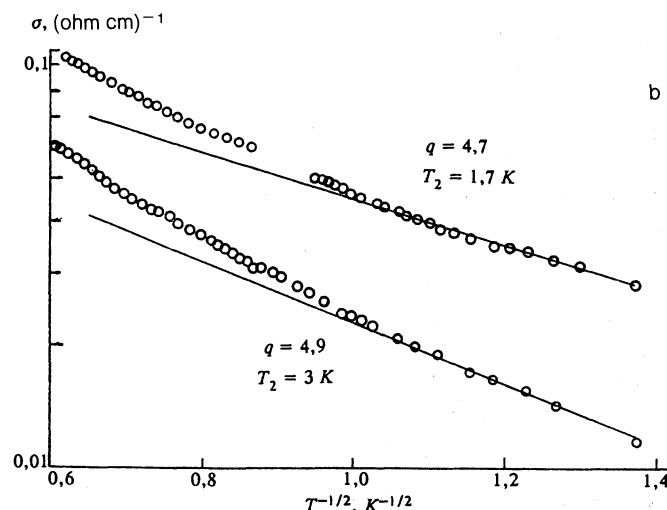
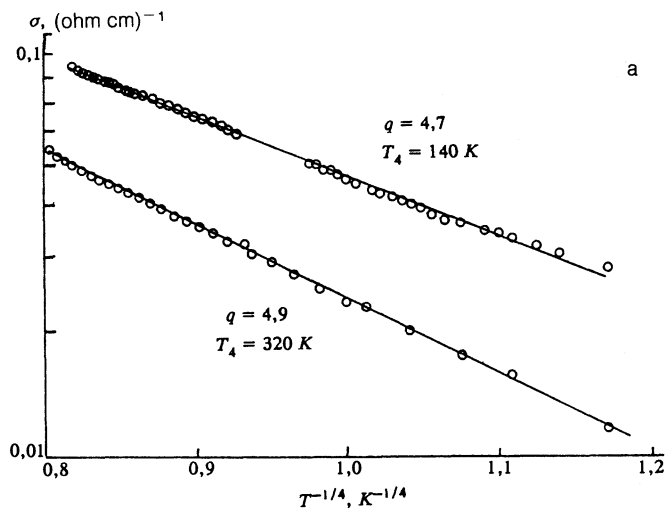


FIG. 5. The same as in Fig. 3 in coordinates a)  $\ln \sigma, T^{-1/4}$  and b)  $\ln \sigma, T^{-1/2}$ .

naturally raises some purely experimental problems and it would certainly be helpful to perform a more detailed study of the same material and to confirm the above result for others. However, it is theoretical questions which are more important to answer, and these are: How can the critical regime be possibly realized in a clustered medium, and precisely what is the meaning of the negative constant  $a$  in (15)?

### 5. UPPER BOUNDARY OF THE CRITICAL REGION

The expressions (10)–(12) for the conductivity in the critical region were derived under the assumption that the  $e$ - $e$  interaction predominates. This manifests itself in that Eqs. (8) and (9) are solved self-consistently and that no *ad hoc* diffusion mechanism has been forced onto the system. It is tacitly assumed that the diffusion of electrons is due to the fluctuations of the same electric field that determines the interaction between the electrons. With rise of temperature, a natural limit is encountered to the validity of such a model. The quantity  $L_{ee}$ , which has the meaning of the diffusion length and decreases with increasing  $T$ , can never become less than  $l$ , the mean free path due to structural inhomogeneities.<sup>11</sup> Although such an  $l$  must exist, how and if it can be measured is somewhat unclear considering that of all elec-

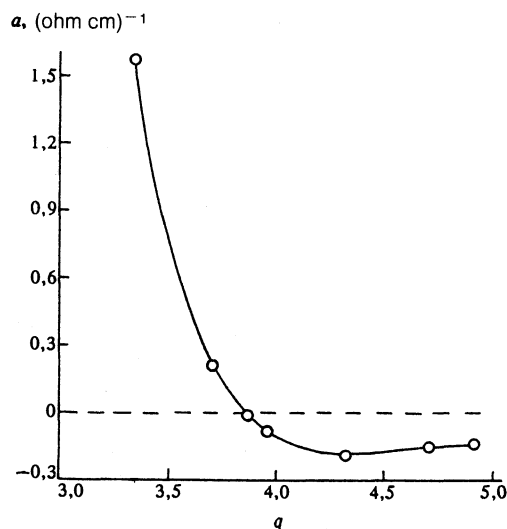


FIG. 6. Nonmonotonic dependence of quantity  $\alpha$ , Eq. (15), on the state parameter  $q$ .

tron gas parameters the only one at our disposal is  $g_F$ , the density of states at the Fermi level. It is probably the existence of an upper temperature bound for the region  $\Delta\sigma \propto T^{1/3}$  which permits an independent measurement of  $l$ .

Using the result of Sec. 3, the condition  $L_{ee} = l$  becomes

$$T = \beta/g_F l^3. \quad (19)$$

The dependence of  $g_F$  and  $l$  on  $f$  (i.e., on  $\xi$ ) is of course different for different materials, but the quantity  $g_F$  is measured independently from the derivative  $\partial\sigma/\partial(T^{1/3})$ .

The preceding discussion does not mean that at  $T > \beta/g_F l^3$  the properties of the material are those of an ordinary metal with  $\partial\sigma/\partial(T) < 0$ . On the contrary, in many cases the growth of  $\sigma$  with temperature is even accelerated. A crossover from  $\sigma \propto T^{1/3}$  to  $\sigma \propto T$  has been observed in  $\text{In}_2\text{O}_x$ ,<sup>4</sup>  $\text{Cd-Sb}$ ,<sup>1</sup> and  $\text{Ge-Au}$ .<sup>17</sup> Reference 1 explains this in terms of the model (8). It is assumed that the inelastic length  $L$  is a combination of two lengths,

$$L^{-1} = L_{ee}^{-1} + L_{in}^{-1}, \quad (20)$$

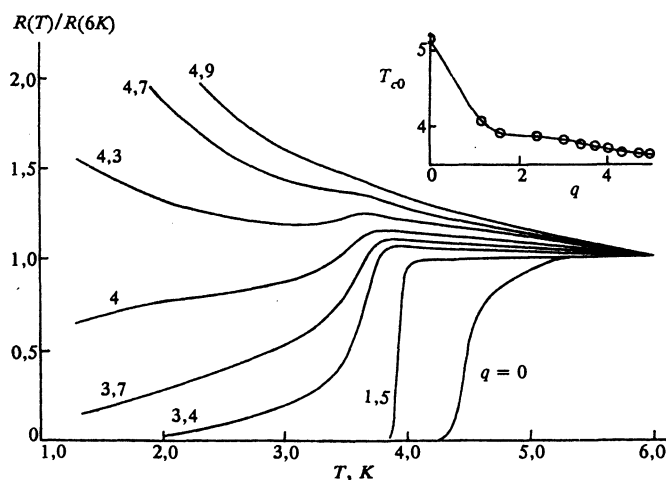


FIG. 7. Evolution of superconducting response over the entire range of states,  $0 \leq q \leq 5$ . Inset: transition onset temperature  $T_{c0}$  as a function of  $q$ .

either of which may decrease down to the limiting value of  $l$ . It follows then that in the high-temperature region the evolution of the system is determined by the length  $L_{in} \propto T^{-1}$ , determined by the inelastic scattering from structural inhomogeneities. It is quite possible that the sum (20) may have more than two terms, each additional term depending on its respective interaction mechanism. We shall not discuss this possibility further, however.

Thus by the upper bound of the critical region we mean that portion of the transition vicinity in which transport properties are dominated by the  $e-e$  interaction. In Cd-Sb this boundary is at about 40 K, which agrees to within an order of magnitude with results on amorphous materials<sup>17,21</sup> and oxides.<sup>4</sup> In materials based on doped  $A^3B^5$  compounds this boundary passes at much lower temperatures of about 1 K,<sup>5,6,22</sup> whereas in doped-silicon-based materials it is not possible at all to identify a critical region with predominant  $e-e$  interaction.<sup>23-25</sup>

### 6. SUPERCONDUCTING INTERACTION AND THE LOWER TEMPERATURE PART OF THE $(f, T)$ -DIAGRAM

The metastable metallic phase of  $Cd_{43}Sb_{57}$  has a superconducting transition at  $T \approx 5$  K. The evolution of this transition at various amorphization stages of the material has been studied in Ref. 2 and it is of interest to plot this evolution in our  $(f, T)$ -diagram. It must be emphasized that the material under study has no large-scale concentration fluctuations (see Sec. 2 above), and is a 3D material in which the superconducting interaction near the MI transition manifests itself in an essentially different manner<sup>26,27,2</sup> than in a 2D material.<sup>28,29</sup>

We may summarize as follows those  $S$ -state results which are relevant to our diagram.

As the localization threshold is approached the  $S$  transition is gradually washed out and on the  $I$  side the resistivity does not vanish at all with decreasing temperature. We note, however, that the kink at the onset of the transition remains observable even further on in the  $I$  region and is virtually unchanged on the  $R(T)$  curve. This is readily seen on the graphs of Fig. 7. It appears that instead of an  $S$  state it is more appropriate to speak of the  $S$  response of the material when it is "switched on" at a certain temperature  $T_{\infty}$ .

The finite resistance observed at  $T < T_{\infty}$  may simply be attributed to "technological" macroscopic inhomogeneities

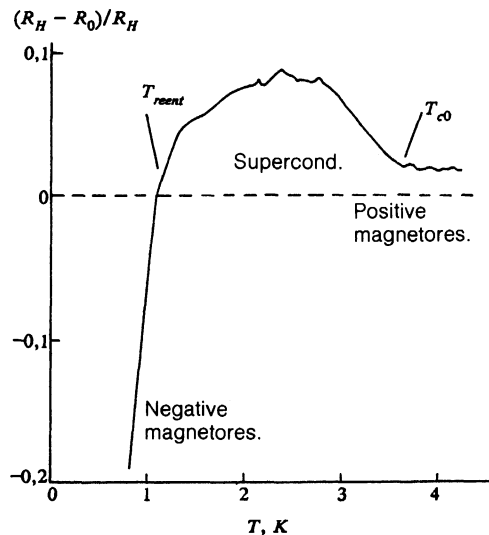


FIG. 8. Magnetoresistivity as a function of temperature in the field  $H = 4$  T for the state  $q = 4.9$ .

in the form of  $S$  enclaves in the normal-metal environment. It is likelier, however, that we are dealing with "physical" inhomogeneities due to the phase stratification of the material on the electronic level. The theoretical premises for this stratification idea can be found in Refs. 30-32.

Experimental evidence in favor of this hypothesis comes from the temperature dependence of the magnetoresistance  $R_H(T)$ . In terms of the macroinclusion model, the destruction of the superconducting inclusions by the field at  $T < T_{\infty}$  increases the sample resistance by an amount

$$\Delta R \approx R_H(T) - R_0(T),$$

dependent on the fractional volume of the  $S$  phase. But as the temperature is lowered, it would appear that  $\Delta R(T)$  can only increase, whereas we see that in  $q > 4$  states it not only passes through a maximum but even changes sign with further decrease (Fig. 8). This means that at low temperatures the system ceases to exhibit a superconducting response with a reduced zero-magnetic-field resistivity—i.e., that a reentrant transition has taken place.<sup>27</sup>

As a characteristic temperature by which to mark the reentrant transition, we may take  $T_{reent}$  at which  $\Delta R(T) = 0$ . Strictly speaking, the  $T_{reent}$  so defined should

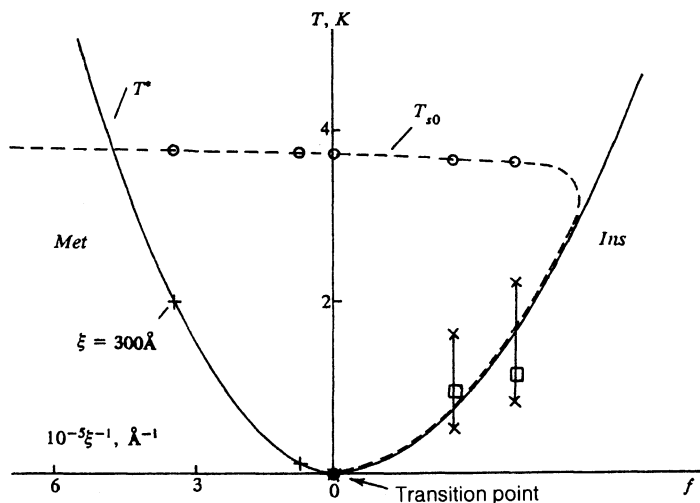


FIG. 9. Low-temperature part of the  $(f, T)$ -diagram. The  $\xi$  scale refers only to the negative half-axis,  $f < 0$ . +: results obtained by comparing experimental curves with the universal curve of Fig. 2; x: results from Fig. 3; o: values of  $T_{\infty}$  (see inset in Fig. 7); □: values of  $T_{reent}$  (see Fig. 8).

be dependent on  $H$ , but this dependence is unlikely to be of importance. The key features of the  $\Delta R(T)$  curve are contained in  $R_0(T)$ , the  $R_H(T)$  curve playing the role of the smooth part of  $\Delta R(T)$ . It is for this reason that the quantity  $\Delta R(T)$  of Fig. 8 is normalized with respect to  $R_H$  rather than to  $R_0$ .

We now turn to the low-temperature part of the  $(f, T)$ -diagram, see Fig. 9.

Since  $\sigma(0)$  yields  $\xi$  through Eq. (7) in the  $M$  part of the scaling region, we employ transverse Ångströms to graduate the left half-axis of the diagram. It is this scale which was used to fit the experimental points to the  $T^*$  curve (two crosses on the plot representing points for which  $T^* < 6$  K).

This scale does not pertain to the right ( $f > 0$ ) side of the diagram. The only assertion to make here is that the points marking the characteristic temperatures of an individual state are all located on a common vertical line. Shown on the diagram are points for two states with  $q = 4.7$  and  $q = 4.9$ . The vertically connected pairs of crosses are taken from the graphs of Fig. 3, the upper points corresponding to the temperature at which a systematic departure of experimental points from a straight line starts to be observed (see vertical bars in Fig. 3). The lower points are determined from intersections of the (extrapolated) straight lines  $\sigma(T^{1/3})$  with the  $T^{1/3}$  axis. The scatter so obtained shows the experimental uncertainty in estimating the lower bound of the scaling region in the  $I$  portion of the diagram.

The dashed curve in Fig. 9 fits the points obtained for the  $S$  state. The upper and lower parts of the curve respectively locate the points  $T_{c0}$  (circles) and  $T_{reent}$  (squares). There is no real significance in that the lower branch of this curve coincides with the solid dividing line between the critical and hopping regions. This simply reflects the suggestion<sup>2</sup> that the superconducting response should vanish when conduction by hopping becomes predominant. As shown in Fig. 9, this suggestion is not inconsistent with experiment.

## 7. CONCLUSIONS

The behavior of conductivity near the MI transition is strongly dependent on the inelastic electron interaction dominating in the system. When subject to an amorphization process, the Cd–Sb alloy offers an example of a three-dimensional material with the  $e$ – $e$  interaction controlling the transition vicinity. In the scaling region, the temperature dependence of  $\sigma$  is given by Eq. (15), i.e.,  $\Delta\sigma \propto T^{1/3}$ . As the temperature is reduced, this gives way either to Eq. (13) on the  $M$  side ( $\Delta\sigma \propto T^{1/2}$ ) or to Eq. (4) type behavior on the  $I$  side (hopping-conduction exponential). Cd–Sb is one of those materials in which the scaling region manifests itself at relatively high temperatures,<sup>4,17,21</sup> so that in principle the above changes in temperature dependences may be studied on either side of the transition. In practice, however, this can only be done in a magnetic field  $H > 4$  T, because at weaker fields the superconducting interaction comes into play at  $T < 4$  K. On the other hand, this adds the evolution of the superconducting response near the MI transition to the range of problems amenable to study on this particular material.

Theoretical studies<sup>33–35</sup> on the superconducting transition temperature  $T_c$  near the Anderson transition have shown a degradation of superconductivity, i.e., a depression of  $T_c$  with increasing disorder. Referring to our  $(f, T)$ -dia-

gram, this means that as  $f$  increases,  $T_c$  should decrease until it eventually vanishes. It is assumed in Refs. 33–35 that the  $S$  state remains homogeneous near the Anderson transition. In an alternative scenario<sup>30,31</sup> we envisage a loss of homogeneity by the  $S$  state close to the MI transition, followed by phase stratification of the system on the electron level. This may probably explain the existence of two branches, with  $T_c \equiv T_{c0}$  and  $T_c \equiv T_{reent}$ , on the  $T_c(f)$  curve for Cd–Sb. An immediate experimental problem which then arises is elucidating the as yet unknown nature of the states in between the branches.

The authors are grateful to A. G. Aronov and D. E. Khmel'nitskiĭ for instructive discussions on the problem, and to E. G. Ponyatovsky for his interest in the work.

<sup>1</sup>V. M. Teplinskii, V. F. Gantmakher, and O. I. Barkalov, Zh. Eksp. Teor. Fiz. **101**, 1698 (1992) [Sov. Phys. JETP **74**, 905 (1992)].

<sup>2</sup>V. F. Gantmakher, V. N. Zverev, V. M. Teplinskii, and O. I. Barkalov, Pis'ma Zh. Eksp. Teor. Fiz. **56**, 311 (1992) [JETP Letters **56**, 309 (1992)].

<sup>3</sup>T. G. Castner, in *Hopping Transport in Solids*, ed. by M. Pollak and B. I. Shklovskii, North-Holland (1991), p. 1.

<sup>4</sup>Y. Imry and Z. Ovadyahu, J. Phys. C **15**, L 327 (1982).

<sup>5</sup>M. C. Maliepaard, M. Pepper, R. Newbury *et al.*, Phys. Rev. B **39**, 1430 (1989).

<sup>6</sup>M. C. Maliepaard, M. Pepper, R. Newbury, and G. Hill, Phys. Rev. Lett. **61**, 369 (1988).

<sup>7</sup>E. Abrahams, P. W. Anderson, D. C. Licciardello, and T. V. Ramakrishnan, Phys. Rev. Lett. **42**, 673 (1979).

<sup>8</sup>P. W. Anderson, Phys. Rev. **109**, 1492 (1958).

<sup>9</sup>N. F. Mott, *Metal-Insulator Transitions*, 2nd ed., Taylor & Francis, 1990.

<sup>10</sup>Y. Imry, J. Appl. Phys. **52**, 1817 (1981); Phys. Rev. Lett. **44**, 469 (1980).

<sup>11</sup>B. L. Altshuler and A. G. Aronov, in *Electron-Electron Interactions in Disordered Systems*, ed. by A. L. Efros and M. Pollak, North-Holland, Amsterdam (1985), p. 1.

<sup>12</sup>N. F. Mott, J. Non-Cryst. Solids **1**, 1 (1968).

<sup>13</sup>A. L. Efros and B. I. Shklovskii in *Electron-Electron Interactions in Disordered Systems* (Ref. 11) p. 409.

<sup>14</sup>E. G. Ponyatovsky and O. I. Barkalov, Mater. Sci. Rep. **8**, 147 (1992).

<sup>15</sup>N. F. Mott and E. A. Davis, *Electronic Processes in Non-Crystalline Materials*, Clarendon Press, Oxford (1971).

<sup>16</sup>A. Kawabata, J. Phys. Soc. Japan. **34**, 2169 (1984).

<sup>17</sup>B. W. Dodson, W. L. McMillian, J. M. Mochel, and R. C. Dynes, Phys. Rev. Lett. **46**, 46 (1981).

<sup>18</sup>K. J. Friedland, A. N. Ionov, R. Rentzch *et al.*, J. Phys.: Cond. Matter **2**, 3759 (1990).

<sup>19</sup>D. M. Finlayson, J. Phys.: Cond. Matter **3**, 3331 (1981).

<sup>20</sup>K. M. Abkemeier, C. J. Adkins, R. Asal, and E. A. Davis, J. Phys.: Cond. Matter (1992) (to be published).

<sup>21</sup>N. Nishida, T. Furubayashi, M. Yamaguchi *et al.*, Solid State Electron. **28**, 81 (1985).

<sup>22</sup>D. L. Newson and M. Pepper, J. Phys. C **19**, 3983 (1986).

<sup>23</sup>W. N. Shafarman, D. W. Koon, and T. G. Castner, Phys. Rev. B **40**, 1216 (1989).

<sup>24</sup>J. C. Phillips, Europhys. Lett. **14**, 367 (1991).

<sup>25</sup>P. Dai, Y. Zhang, and M. P. Sarachik, Phys. Rev. Lett. **66**, 1914 (1991).

<sup>26</sup>M. Kunchur, P. Lindenfeld, W. L. McLean, and J. S. Brooks, Phys. Rev. Lett. **59**, 1232 (1987).

<sup>27</sup>M. Kunchur, Y. Z. Zhang, P. Lindenfeld *et al.*, Phys. Rev. B **36**, 4062 (1987).

<sup>28</sup>D. B. Haviland, Y. Liu, T. Wang, and A. M. Goldman, Physica B **169**, 238 (1991).

<sup>29</sup>T. Tamegai, K. Koga, K. Suzuki *et al.*, Jpn. J. Appl. Phys. **28**, L 112 (1989).

<sup>30</sup>L. N. Bulaevskii, S. V. Panyukov, and M. V. Sadovskii, Zh. Eksp. Teor. Fiz. **92**, 672 (1987) [Sov. Phys. JETP **65**, 380 (1987)].

<sup>31</sup>A. A. Gorbatshev, Yu. V. Kopaev, and I. V. Tokatly, Zh. Eksp. Teor. Fiz. **101**, 971 (1992) [Sov. Phys. JETP **74**, 521 (1992)].

<sup>32</sup>M. V. Sadovskii, in *Studies of High- $T_c$  Supercond.*, ed. by A. V. Narlikar, Nova Sci. Publ., New York (1992).

<sup>33</sup>M. Ma and P. A. Lee, Phys. Rev. B **32**, 5658 (1985).

<sup>34</sup>T. K. Ng, Phys. Rev. B **43**, 10204 (1991).

<sup>35</sup>T. R. Kirkpatrick and D. Belitz, Phys. Rev. Lett. **68**, 3232 (1992).

Translated by E. Strelchenko